Environment, Development and Sustainability (2022) 24:9963–9984
https://doi.org/10.1007/s10668-021-01852-9

Comparative evaluation of cellulose nanocrystals from bagasse and coir agro-wastes for reinforcing PVA-based composites

Krishnavani Pavalaydon[1] · Hareenanden Ramasawmy[2] · Dinesh Surroop[1]

Received: 17 May 2021 / Accepted: 20 September 2021 / Published online: 5 October 2021

Abstract
In order to increase resilience of planters against climate change and bring additional economic benefits, agro-wastes can be exploited for extracting nanocellulose to produce eco-friendly composites. This paper focused on extracting nanocellulose from sugarcane bagasse and coir (*cocos nucifera*) using chemical methods including mercerisation, bleaching and acid hydrolysis. Taguchi Design of Experiment showed that the optimum alkaline treatment conditions of bagasse were at 2 wt% NaOH at 90 °C for 16 h. The morphological changes occurring along each treatment stage were observed using Fourier-Transform Infrared spectroscopy and Scanning Electron Microscopy. The differences in the nanoparticles extracted from the two biomass were studied through the determination of crystallinity indexes and particle size. Cellulose nanocrystals (CNCs) from coir exhibited a total crystallinity index (TCI) of 1.03 and an average particle size of 137.3 nm while CNCs extracted from sugarcane bagasse under similar treatment conditions had a TCI of 0.85 and an average particle size of around 48 µm. Dynamic Light Scattering findings showed risks of agglomeration after freeze drying. Bio-nanocomposite films with polyvinyl alcohol (PVA) as matrix were manufactured by the solvent casting process. The highest tensile strength (38.2 MPa) was obtained for CNCs extracted from coir at a CNC/PVA loading of 0.5 wt%, representing a 96.9% increase in the tensile strength as compared to the unreinforced PVA matrix. This study showed that sugarcane bagasse and coir are suitable sources of nanocellulose and can be used to prepare bio-composites with considerably high tensile strengths.

Keywords Cellulose nanocrystals · Coir (*cocos nucifera*) · SEM · Sugarcane bagasse · Total crystallinity index · Tensile strength

✉ Krishnavani Pavalaydon
pavalaydonkrishnavani@gmail.com

[1] Department of Chemical and Environmental Engineering, Faculty of Engineering, University of Mauritius, Réduit 80837, Mauritius

[2] Department of Mechanical and Production Engineering, Faculty of Engineering, University of Mauritius, Réduit 80837, Mauritius

1 Introduction

Being a Small Island Developing State (SIDS), Mauritius is not immune to the effects of climate change. Significant impacts on the hydrologic cycle have caused a decrease of about 104 mm in the mean annual rainfall in the last 70 years between 1951 and 2020 around the island, with a decrease of around 8% over the last decade. (Mauritius Meteorological Services, 2021). The projected decline in rainfall and increase in evapotranspiration may lead to a reduction in agricultural production by as much as 15–25% by 2050 (Ministry of Environment, Solid Waste Management and Climate Change, 2021). Indeed, the decrease in rainfall has led to many farmers abandoning their fields due to lack of income from the sale of less produce. This is causing a problem of food security where the country has to even import vegetables to cater for lack of local produce. Indeed, the value of imports of vegetables to Mauritius has increased progressively over the last few years from $ 95 thousand in 2017 to $ 102 thousand in 2018, $ 115 thousand in 2019 and $ 131 thousand in 2020 (TrendEconomy, 2021). Therefore, there is a need to increase the resilience of planters against the adverse effects of climate change. Two potential ways of doing so include either changing the agricultural practices or finding new ways to increase income such as manufacturing high value products from agro-wastes resulting from industrial crops. This can address the problem of waste management as well (Chen et al., 2016).

Over the past decade, concerns related to the alarming impacts of global warming and depletion of non-renewable resources have contributed to the exploitation of the abundant renewable resource of agro-wastes or biomass wastes, such as sugarcane bagasse and forest residues, for bioenergy production (Yu et al., 2021). With a view to tap into the full potential of agro-wastes, researchers have further explored the use of such versatile material in diverse highly valued applications including biofuel production, biodegradable packaging materials and biomass composites used as adsorbent of water pollutants and dyes (Basri et al., 2019; Yadav et al., 2021; Yu et al., 2020a, b, 2021).

However, the undesirable properties of lignocellulosic material, such as high water absorption and poor thermal stability, limit its prospective applications. Ultimately, increasing attention has been particularly paid to the extraction of nanocellulose from agro-wastes for high-value added applications (Abitbol et al., 2016; Abraham et al., 2011; Rasheed et al., 2020). Due to its remarkable features such as high mechanical strength, high length-to-diameter ratio, high crystallinity and several hydroxyl groups, nanocellulose has attracted much interest in a vast spectrum of applications ranging from composite materials to biomedical engineering (Jahan et al., 2018; Nasir et al., 2017). The addition of nanocellulose as filler material to reinforce biopolymers such as polylactic acid (PLA) or polyvinyl alcohol (PVA) has also paved the way for the use of nanocomposites in various industrial applications such as primary packaging materials, films and foams, surface modified composite materials, tissue engineering scaffolds, fire-resistant nanocomposites and CO_2 separation membranes (Abdullah et al., 2021; Ilyas et al., 2021; Jahan et al., 2018).

Common lignocellulosic biomass crops that can be used for extraction of nanocellulose in Mauritius include agro-wastes such as sugarcane bagasse, banana pseudostems, coconut coir, pineapple leaves/peels, maize stover, grass/ornamental crops such as elephant grass and vacoas plant (*Pandanus utilis*). Sugarcane bagasse is currently being used for cogeneration along with coal to produce both heat and electricity. However, the sugar sector is no longer as profitable as before, due to the liberalization by EU of the Mauritian quotas which led to a drop in the international market price of locally produced sugars (Mauritius Sugar Syndicate, 2018). As such, many planters are abandoning their sugarcane

fields. Considering the fact that Mauritius has a good solar regime and given that the price of electricity from solar has decreased and is expected to decrease further (International Renewable Energy Agency, 2018), solar energy can therefore play an important role in the energy mix of the country whereby it can replace bagasse. Bagasse can hence be exploited for other purpose to produce high value-added products. The agro-wastes generated from other crops are not being extensively used in Mauritius and are mostly burn in the fields or disposed in the environment to degrade. Similarly, coconut coir is disposed as waste and end up in the only sanitary landfill of the country, which is about to saturate soon. The total amount of solid wastes landfilled in 2020 exceeded 500,000 tonnes and this figure is projected to go up to 600,000 tonnes by 2030 on a business-as-usual scenario (Ministry of Environment, Solid Waste Management and Climate Change, 2021). Given that Mauritius is a SIDS, it has limited land and cannot afford to have another landfill, there is an urgent need to divert these wastes from the landfill by converting the wastes into useful resources to be in line with circular economy. In line of the above concern, the Ministry of Environment, Solid Waste Management and Climate Change has fixed an exceptionally ambitious target of 70% of waste diversion from landfilling by 2030. Furthermore, the Government of Mauritius has banned the use of non-biodegradable plastic bags and certain single use non-biodegradable plastic products as from March and April 2021 respectively (Ministry of Environment, Solid Waste Management and Climate Change, 2021). Therefore, the extraction of nanocellulose from agro-wastes could offer an interesting opportunity for creating high value-added materials, especially biodegradable products, for several applications; thereby creating new business opportunities for the farmers who are already struggling in this current COVID-19 era.

Several research works have been done on the reinforcement of PVA using nanocellulose extracted from different biomass. Asem et al. (2018) produced biodegradable films by incorporating nanocellulose extracted from sugarcane bagasse into a PVA/starch matrix. They investigated the water absorption properties of the resulting films and found that the lowest water intake of 69.41% could be obtained with 1 wt% nanocellulose loading, 3 g PVA, 1 g starch and 80 ml of water. Similarly, Jahan et al. (2018) investigated the potential use of nanocellulose/PVA membranes in biogas separation. They reported an increase of 9.7% in the rate of moisture uptake as CNC content was increased from 0.5 to 6 wt% at a relative humidity of 93%. The absorption of moisture by the membranes leads to increases in weight as compared to the pure PVA and it occurs due to the hydrophilic nature of nanocellulose. However, at higher CNC levels, CNCs create a reinforcing effect by acting as a cross-binder and hence cause a reduction in swelling of the membranes. The authors hence concluded that low CNC content in CNC/PVA membranes are suitable for providing high permeability for gas separation. Srivastava et al. (2021) recently reported a 14.3% increase in the tensile strength of 20 wt% banana pseudostem short fibre (less than 53 μm) and 3 wt% nanocellulose reinforced PVA composite film (120 μm). These authors reported a much lower tensile strength when 5 wt% nanocellulose was added to the banana short fibre-PVA composite due to significant agglomeration of nanocellulose leading to a non-homogeneous composite. Due to the presence of agglomeration sites within the film, there is less hydrogen bonding interactions with the PVA matrix, which prevent good adhesion or anchoring of the nanocellulose to the matrix. This ultimately leads to the failure of the composite at a lower tensile loading.

However, no study has been observed on the comparison of PVA reinforced nanocomposite films produced using nanocellulose isolated under similar conditions from two different biomass. The amount of cellulose differs for each biomass and nanocellulose extracted from different biomass materials may show variations in terms of shape, size and

crystallinity. These variations can in turn lead to distinct reinforcement effects in polymer matrices. This study was therefore conceived to focus on the comparison of the characteristics of nanocellulose extracted from sugarcane bagasse and coir under similar preparation conditions. There have not been many studies like this in SIDS and therefore it represents an innovative solution to convert agro waste into a useful resource. The cellulose from sugarcane bagasse (SCB) and coir fibre (*cocos nucifera*), which are agro-waste materials, was isolated using alkaline treatment with delignification and was then acid hydrolyzed to isolate nanocellulose. Taguchi Design of Experiment was used to determine an optimum set of conditions for the alkaline treatment of bagasse. The optimum conditions obtained for bagasse were also applied for the pre-treatment of coir fibre for the purpose of comparing nanocellulose and nanocomposite films produced under similar conditions from two different biomass. However, it is understandable that the optimal conditions for the mercerisation process can be different depending on the type of waste. Optimisation of the mercerisation of bagasse was done instead of that of coir, because of the greater availability of bagasse in the country as compared to coir and the comparatively higher cellulose content (44.9–46%) in contrast to that of coir (41.7–44%) makes bagasse a more attractive source of nanocellulose (Fatmawati et al., 2013; Mohomane et al., 2017; Rencoret et al., 2013; Zhao et al., 2008). Solution casting using polyvinyl alcohol as biopolymer reinforced with the nanocrystals was thereafter used to produce biodegradable nanocomposites, which were investigated in term of their tensile strengths. Characterisation of the nanocellulose extracted from the two biomass under similar conditions was used to study their differences in terms of morphology and degree of crystallinity and to explain their consequent effect on the mechanical properties of the resulting nanocomposites.

The Covid-19 pandemic has caused unimaginable ramifications to the economic and social development in Mauritius. For the past 16 months till mid-July 2021, the tourism sector was at a halt with the closure of the national border to international travellers. As a result, the fall in tourism expenditure has indirectly affected the agricultural sector, leading to reduction in earnings of 16%. Many farmers, who were supplying their products to hotels, were having significant difficulties in selling the excess products at a reasonable price. Additionally, with the world on the verge of crossing the dangerous limit of 1.5 °C in average global temperature, Mauritius is likely to face unprecedented challenges from climate change impacts. In line of such harsh situation, there is an urgency to move towards sustainable trajectories that prioritise ecological protection, economic and social prospect. Therefore, accounting the declining profitability from the agricultural sector and loss of useful resources from dumping of agro-wastes, this study provides an appealing and sustainable alternative to tap into the full potential of agro-wastes in SIDS such as Mauritius. This study is also in line with the objective of the SWITCH Africa Green Project by enabling the promotion of a circular business model through valorization of biomass wastes and also contributing to the social development of the country through provision of green job opportunities (Ministry of Environment, Solid Waste Management and Climate Change, 2021).

2 Materials and methods

Materials used included sugarcane bagasse, obtained from a local sugar factory and coir (*cocos nucifera*) from the Northern part of the island.

2.1 Taguchi design of experiment (DoE)

The purpose was to determine an optimum set of parameter conditions for the alkaline treatment process that gives maximum yield of bagasse pulp with nearly complete removal of hemicellulose and lignin. From literature review, the three variable factors identified were concentration of NaOH (purity 98%), time and temperature. The range of conditions showing promising results in terms of mechanical properties of nanocellulose and effective removal of non-cellulosic constituents include concentration of 2–17.5 wt% NaOH, duration of 2–24 h and temperature varying from ambient conditions to 90 °C (Benyahia et al., 2013; Costa et al., 2015; Wulandari et al., 2016). Selection of the second level for each factor was done by considering mercerisation conditions within the above range of values, which were investigated in previous studies and provided favourable results (Dai et al., 2018; Mandal and Chakrabarty, 2011; Trifol et al., 2016; Wulandari et al., 2016). Therefore, the following conditions were investigated: concentration of NaOH (2, 10 and 17.5 wt%), time (1.5, 5 and 16 h) and temperature (room temperature, 45 and 90 °C). The L9 orthogonal array was used with the Nominal-the-best type methodology for calculating the signal to noise (*S*/*N*) ratio.

2.2 Extraction of nanocellulose

2.2.1 Alkaline treatment

The bagasse and coir were dried in the oven at 60 °C for 24 h and then pulverized to a size of < 1.0 mm. The set of experiments for the Taguchi DoE was first carried out on sugarcane bagasse. Dried pulverized bagasse was weighed and treated with NaOH based on a constant fibre to liquor ratio of 1:20. The concentration of NaOH, temperature and duration were set according to the L9 array. After the required treatment time, the treated bagasse was washed until pH became neutral. The bagasse pulp was then dried at 60 °C in the oven for 24 h and the yield of treated bagasse was determined. Each experimental run was carried out twice. Taguchi DoE was then applied to determine an optimum set of conditions (run *A*) based on percentage yield of bagasse pulp. A second set of conditions (run *B*) that resulted in a significantly high Signal to Noise (*S*/*N*) ratio, comparable to that obtained at optimum conditions, was also considered. In the case of the coir fibre, alkaline treatment was carried out at the same set of optimum conditions as those obtained for bagasse, that is, run *A*. The successive steps for extraction of nanocellulose was thus carried out on (1) two samples of mercerised bagasse, treated according to conditions of runs *A* and *B,* respectively, and on (2) one sample of mercerised coir fibre, treated according to run *A*.

2.2.2 Delignification by bleaching

The dried bagasse and coir pulps were soaked in 3 wt% sodium hypochlorite (NaClO) solution at a solid to liquid ratio of 1:10, for about 12–24 h at room temperature until a white coloured pulp was obtained. The bleached bagasse and coir were then washed with distilled water until neutral pH was obtained. Drying for both materials was done at 60 °C for 24 h.

2.2.3 Nanocellulose extraction by acid hydrolysis

Acid concentration, temperature and time are important parameters that need to be controlled during the acid hydrolysis process. The most commonly used conditions are sulfuric acid at a concentration varying around 64 wt%, temperature at 45 °C and reaction time for about 45–60 min. A preliminary test using 64 wt% sulfuric acid (purity 98%) at 45 °C for 45 min under vigorous agitation with a ratio of cellulose to sulfuric acid 1:20 was initially conducted and a brown suspension was obtained, indicating the possible occurrence of other side reactions such as dehydration and oxidation (Börjesson & Westman, 2015; Wulandari et al., 2016). Consequently, the acid hydrolysis was carried out using milder conditions as reported by Mtibe et al. (2015). Sulfuric acid solution at a concentration of 50 wt% was heated to 40 °C and the dried bleached bagasse and coir were added according to a solid/liquor ratio of 1:20. The mixture was hydrolyzed for 30 min at 1000 rpm while ensuring the temperature remained at 40 °C. The reaction was then quenched by adding distilled water and the suspension was centrifuged at 1500 rpm for 30 min. The centrifugation was repeated twice to ensure effective partial removal of sulfuric acid. After centrifugation, the suspension obtained was dialyzed with tap water until it reached neutral pH after three days. The neutral colloidal suspension was sonicated for 5 min at 60% amplitude to produce a stable NC suspension, which was freeze-dried (Fig. 1).

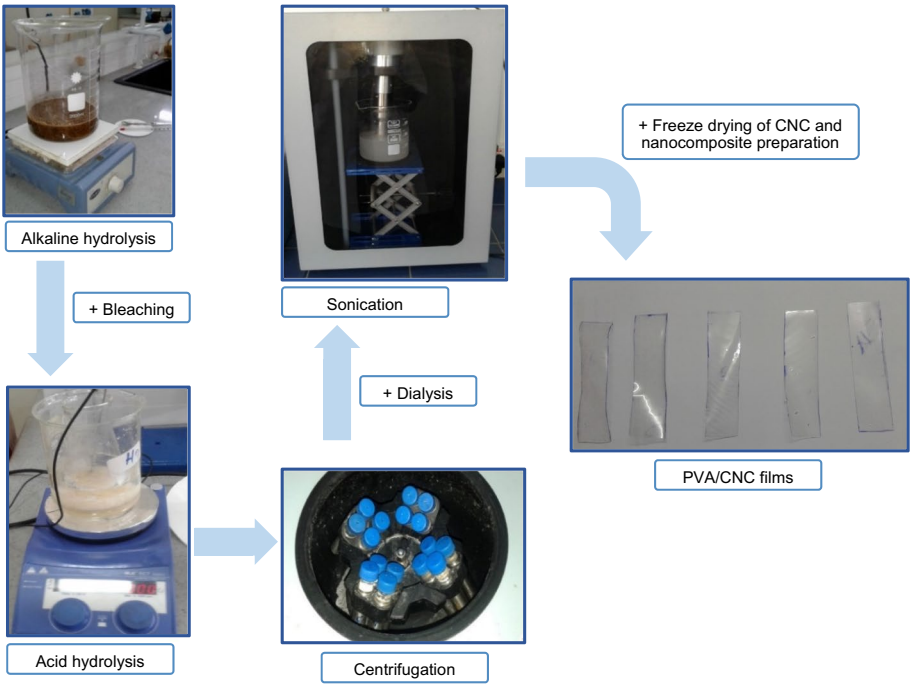

Fig. 1 Treatment procedures performed for the isolation of CNC

2.3 Preparation of CNC/PVA composites through solution casting

Polyvinyl alcohol (PVA17-88S with degree of hydrolysis of 86.0–89.0 mol%) powder was dissolved in distilled water at 80 °C for 2 h under vigorous stirring and then left to cool to ambient temperature under mechanical stirring to produce a 10 wt% PVA solution. Bagasse and coir related nanocellulose suspensions of 2 wt% were also prepared under continuous stirring at room temperature. Small amount of CNC addition to PVA polymer in the range of 0.5–5wt% is reported to be enough to improve the mechanical behaviour of the pure polymer due to their large surface area (Alexandre and Dubois, 2000; Börjesson & Westman, 2015; Peng et al., 2013). Consequently, the weight ratios of CNC addition relative to PVA matrix were chosen at 0.5 and 2 wt%. The wide gap between the 2 values will help to verify whether there is a significant improvement in mechanical performance. CNC/PVA suspensions were then made by mixing 0.5 and 2 wt% CNC relative to weight of PVA solution. The suspensions were sonicated for 5 min at 60% amplitude for homogenization (Zhou et al., 2012) and poured onto the mould for oven-drying at 90 °C for 6 h. The dried films were slowly peeled off from the mould surface for subsequent mechanical testing (Fig. 2).

2.4 Characterisation

2.4.1 Fourier Transform Infrared (FTIR Spectroscopy)

The FTIR spectra of the untreated biomass, treated samples and freeze-dried nanocellulose were obtained using the C-Bruker Alpha Platinum ATR spectrometer in the range of 400–4000 cm^{-1}. FTIR was used to ensure that there was no cellulose degradation during optimisation of alkaline treatment, to study the changes in terms of the removal of non-cellulosic materials occurring along each treatment stage and to compare the nanocellulose extracted from coir and bagasse under similar conditions. The following three crystallinity indices were also evaluated by first applying baseline correction to normalise

Fig. 2 Products obtained after each treatment applied to untreated sugarcane bagasse and coir fibre

the absorbance spectra and then determining the relevant peak heights (A) at the specific wavelengths (Ciolacu et al., 2011; Khai et al., 2017; Poletto et al., 2013):

- Total crystalline index, $\mathrm{TCI} = \frac{A_{1371}}{A_{2901}}$
- Lateral order index, $\mathrm{LOI} = \frac{A_{1420}}{A_{893}}$
- Hydrogen bond intensity, $\mathrm{HBI} = \frac{A_{3350}}{A_{1318}}$

Due to the presence of both crystalline and amorphous regions in the spectrum, FTIR gives only relative values. The most common method to ensure the accurate evaluation of the crystallinity indices would be X-Ray Diffraction, whereby the peak height method is usually used (Park et al., 2010). However, due to the unavailability of an X-Ray Diffractometer, the FTIR was chosen. According to Liu (2013), a high value of $R^2 = 0.97$ was obtained for the correlation of crystalline indices by FTIR with that of XRD.

2.4.2 Scanning electron micrographs (SEM)

SEM analysis, using VEGA3 TESCAN with gold/palladium coating, was used to investigate the changes in the morphological structures of the fibre along each treatment stage. For nanocellulose observation, a suspension of 0.002 wt% in acetone was prepared under mechanical stirring.

2.4.3 Dynamic light scattering (DLS)

DLS was used to determine the relative average size of nanocellulose particles of bagasse and coir. 0.1 wt% nanocellulose suspension was made by dissolving in distilled water under continuous stirring. The suspension was then placed in the Brookhaven 90Plus Particle Size Analyser using a laser output power of 35 mW at scattering angles of 15° and 90°.

2.5 Determination of tensile strength of the reinforced bioplastic

Tensile testing of PVA films reinforced with CNCs was performed as per ASTM D882-12 standard. The PVA and CNC/PVA films were cut in rectangular shapes of length 100 mm and width 25 mm. The test parameters were adjusted as follows: load cell of 500 kN, grip distance of 50 mm and crosshead speed of 500 mm/min. For each weight ratio of CNC/PVA composite film, 5 samples were tested (Table 1).

3 Results and discussions

3.1 Selection of an optimum set of conditions for alkaline treatment

The quality characteristic chosen under the Taguchi analysis was the maximization of the yield of bagasse pulp after mercerisation treatment. The highest signal to noise ratio ($\eta = 38.2$ dB) based on yield was found to be obtained at NaOH concentration of 2 wt% at room temperature for 1.5 h. As can be observed in Table 2, the analysis of variance (ANOVA) showed that concentration of NaOH solution was the most dominant parameter since it accounted for the largest sum of squares. The effect of each parameter was then

Table 1 Calculated S/N ratios based on yield

Expt No.	Factor assigned			Yield		Mean yield μ	SDV σ	S/N ratio (η)
	concentration (wt %)	Time (h)	Temperature (°C)	Y_1	Y_2			
1	2	1.5	Room temp	77.33	76.00	76.67	0.943	38.20
2	2	5	45	78.00	72.33	75.17	4.007	25.46
3	2	16	90	54.33	53.00	53.67	0.943	35.11
4	10	1.5	45	43.67	54.33	49.00	7.542	16.25
5	10	5	90	26.67	44.00	35.33	12.257	9.20
6	10	16	Room temp	39.67	48.33	44.00	6.128	17.12
7	17.5	1.5	90	44.67	46.67	45.67	1.414	30.18
8	17.5	5	Room temp	52.33	48.67	50.50	2.593	25.79
9	17.5	16	45	43.00	41.67	42.33	0.943	33.05

Table 2 Sum of squares of each factor in ANOVA analysis

Factor	Degrees of freedom	Sum of squares	Mean sum of squares	F	Per cent of variation (%)
A. Concentration	2	601.21	300.61	62.4	79.7
B. Time	2	133.51	66.75	13.8	17.7
C. Temperature	2	9.38	4.69	–	1.2
Interaction	2	9.89	4.95	–	1.3
Total	8	753.99	–		–
Pooled error	4	19.27	4.82	–	–

evaluated in terms of their deviation from the overall mean. The optimum level for each factor is reflected by the highest signal to noise ratio, and is obtained as follows: NaOH concentration of 2 wt%, soaking time of 16 h and a temperature of 90 °C. This implied that the combination of these optimum factor levels (run *A*) would give the optimum cellulose yield with almost complete removal of lignin and hemicellulose. Since this combination was already conducted in the experimental run 3 as shown in Table 1, there was no need for any confirmatory test. It was also observed that a significantly high signal to noise ratio was obtained at NaOH concentration of 17.5 wt%, soaking time of 1.5 h and a temperature of 90 °C (run *B*).

3.2 Yield of nanocellulose from sugarcane bagasse (SCB)

An average nanocellulose yield of 35% from bagasse was obtained. A similar yield value (36%) was reported by Mtibe et al. (2015) extracting CNC from maize stalk residues under similar acid hydrolysis conditions. Hafemann et al. (2019) and Kargarzadeh et al. (2012) both investigated the effect of varying acid hydrolysis conditions on yield of CNC produced and reported that low yields in the range of 7.8–23% may be attributed to the degradation of the crystalline cellulose structures during the reaction under harsher conditions. The potential of using SCB to extract nanocellulose instead of burning it with coal

to generate electricity was assessed by a simple cost analysis. Using an annual production rate of bagasse of around 360,000 tonnes obtained from a local sugar industry at an average moisture content of 49.4% (Omnicane, 2017), the resulting annual production rate of nanocellulose was determined at around 63,700 tonnes using the average nanocellulose yield of 35% and the associated income was evaluated at around US$ 255 million. Considering the case where bagasse is to be exclusively used for the production of nanocellulose, an additional amount of coal is required to be used as fuel in lieu of bagasse. Around 322,000 tonnes of coal is used to provide for 444 GWh of electricity in the usual case scenario (Omnicane, 2017). The additional amount of coal required to provide for the remaining 143 GWh that is normally provided by bagasse amounted to around 104,000 tonnes. Accordingly, the expense associated with purchasing additional coal was found to be at around US$ 7 million. Taking into account the income that can be derived from the nanocellulose production and the expenses associated with the fuel change, the projected gross profit was estimated to be around US$ 248 million. Given that the sugar industry in Mauritius is currently struggling to compete on the global market, this new venture of extracting nanocellulose from sugarcane bagasse may prove to be beneficial, in the future with further advancement in nanocellulose technology, to re-engineer the sugar sector. It will also act as incentive for small-scale farmers to avoid abandoning their sugarcane plantations, as has been the case in recent years in Mauritius.

3.3 FTIR analysis

3.3.1 FTIR characterisation of mercerised samples

In order to ensure that optimum cellulose yield was obtained at the optimum set of conditions of NaOH concentration of 2 wt%, soaking time of 16 h and at temperature of 90 °C, the band at 1728 cm^{-1} was considered and its corresponding band area was defined after applying baseline correction to normalise the spectra. The band at 1728 cm^{-1} corresponded to the groups of hemicellulose or ester linkage of carboxylic acids of lignin and/or hemicellulose and this band decreased in intensity after alkaline treatment, showing complete removal of hemicellulose and partial removal of lignin. On the other hand, lignin was not completely removed after alkaline treatment since there were bands at 1550–1600 cm^{-1}, which corresponded to the aromatic C=C ring vibration due to presence of lignin. It was hence observed that the band at 1728 cm^{-1} was not present for the two experimental combinations: runs *A* and *B*. Similarly, upon mercerisation of coir fibre at experimental conditions of run A, the disappearance of the band at 1728 cm^{-1} indicated complete removal of hemicellulose.

Upon alkaline treatment, there is also conversion of cellulose I (natural cellulose) to cellulose II, which thereby infers that cellulose II is more stable than cellulose I (Dinand et al., 2002). This was indicated by the increase in band intensity near 895 cm^{-1}, which corresponded to cellulose II. The transformation from the parallel chain structure of cellulose I to the more stable anti-parallel chain structure of cellulose II would consequently affect the mechanical properties of the fibre. A shift in the significant bands related to the presence of cellulose I, namely at around 2900 cm^{-1}, attributed to the aliphatic –CH stretching and 1420 cm^{-1},assigned to the in-plane bending of the hydroxyl group, was also observed, thereby indicating the transition to cellulose II (; Majid et al., 2017). Duchemin (2015) obtained similar findings by performing the mercerisation of cellulose. A transition

to cellulose II was observed as the band at 1420 cm^{-1} of the untreated cellulose shifted to 1419 cm^{-1} upon mercerisation (Fig. 3).

3.3.2 FTIR characterisation of bleached, acid hydrolysed and nanocellulose samples

Characteristic bands representing lignin in untreated bagasse and coir fibres included a band at 1240 cm^{-1} attributed to the aromatic C–O–C stretching and bands at around 1510 and 1603 cm^{-1} assigned to the aromatic C=C skeletal vibration (Abraham et al., 2013; Feng et al., 2018; Wulandari et al., 2016). These bands disappeared after bleaching of the mercerised bagasse and coir samples, indicating removal of lignin.

The acid hydrolysed and nanocellulose samples of both bagasse and coir fibres gave similar spectra as their respective bleached samples since their chemical compositions are identical. There were also no new functional groups in the acid hydrolysed and nanocellulose samples, thus implying no new bond formation during acid hydrolysis.

Comparing the IR spectra of the nanocellulose samples, it could be observed that the band intensities at 3330 cm^{-1} and at 1029 cm^{-1} were higher for nanocellulose extracted from coir as compared to that extracted from bagasse under similar conditions (run *A*). The broad band at 3330 cm^{-1} corresponded to the exposed hydroxyl groups of cellulose, which are bound by intermolecular hydrogen bonding (Abraham et al., 2013), while the band at 1029 cm^{-1} is associated with the –C–O stretching of cellulose. The presence of these functional groups are essentially responsible in promoting hydrogen bonding, which is the major force of attraction in ensuring the interaction between nanocellulose and PVA matrix for good adhesion and dispersion. Jahan et al. (2018) analysed the IR spectra of PVA/CNC nanocomposites membranes at different CNC loadings and found that the band associated with the free O–H stretching vibration of –OH groups was present in all spectra and was due to the intermolecular hydrogen bonding

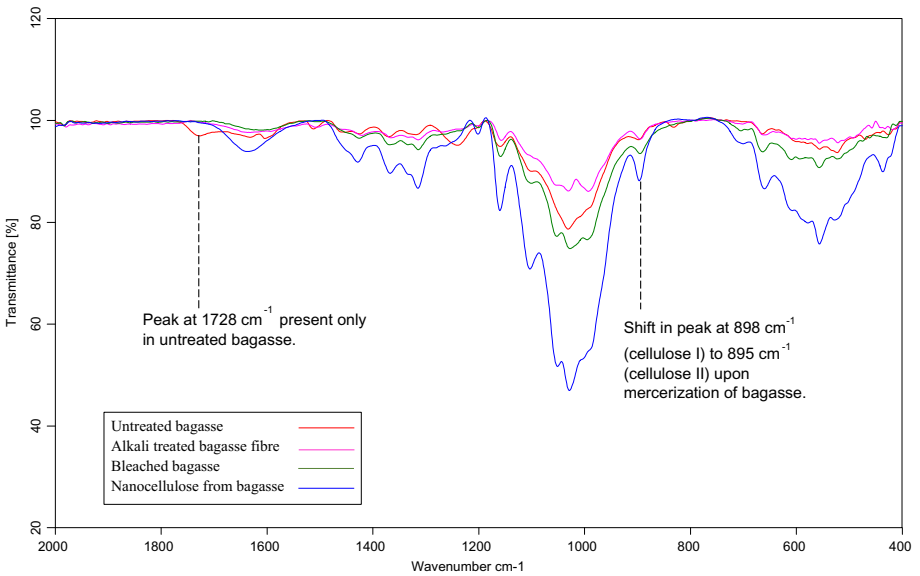

Fig. 3 IR spectrum of untreated bagasse, alkali-treated bagasse (run *A*), bleached bagasse and nanocellulose from bagasse

between hydroxyl groups of PVA and CNC and the intramolecular hydrogen bonding within PVA. The authors also reported that the wavenumber associated with this band increased with increase in CNC loading. At 4 wt% of CNC addition, the wavenumber was around 3331 cm^{-1} compared to 3292 cm^{-1} at 1 wt% CNC and 3285 cm^{-1} of pure PVA. The authors hence concluded that such variations were due to possible interactions between PVA and CNC. Likewise, Jayaramudu et al. (2018) reported that addition of 3 wt% of CNC caused the O–H stretching vibration band to shift to 3402 cm^{-1} from 3422 cm^{-1} of pure PVA due to overlapping of the intermolecular hydrogen bonded –OH groups in PVA and CNC.

These previous studies indicate interactions between CNC and PVA occur mainly due to the presence of functional groups promoting hydrogen bonding. The higher band intensities at 3330 cm^{-1} and 1029 cm^{-1} of nanocellulose from coir as compared to that from bagasse hence suggested that the former would serve as better reinforcing agents in PVA matrix (Fig. 4).

It was also noted that the IR spectra of the untreated and treated bagasse and coir samples all showed a broad band at 3000–3500 cm^{-1} that corresponded to free O–H stretching vibration due to the presence of OH groups in cellulose. Similarly, the following bands were also present in all spectra: a band at around 2900 cm^{-1} indicating the C–H stretching vibration of alkyl groups and a band at 1644 cm^{-1} attributed to the O–H bending vibration of adsorbed water by hydrophilic groups.

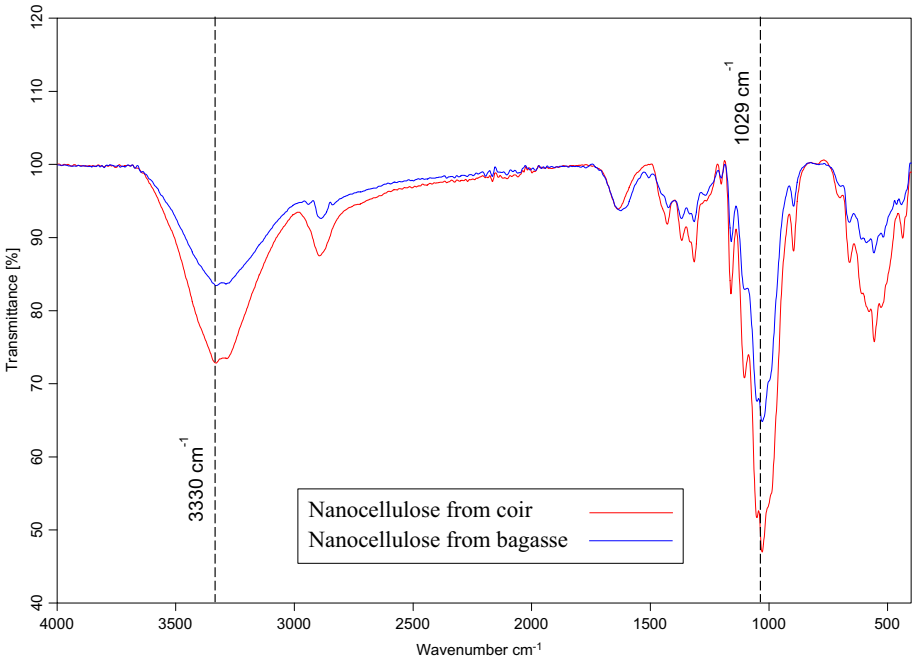

Fig. 4 IR spectrum of nanocellulose samples from coir and bagasse respectively (run *A*)

3.3.3 Crystallinity indices

Hemicellulose and lignin display amorphous structures while cellulose can exist in crystalline form due to the presence of hydrogen bonding in its molecular structure. Thus, any changes in the biomass morphology and composition can be detected through variations in the crystallinity of the cellulose fibres (Feng et al., 2018). In this respect, the IR spectra of the samples were used to evaluate the TCI, LOI and HBI and the obtained results are displayed in Table 3.

The degree of crystallinity is reflected by the total crystalline index (TCI) (Poletto et al., 2013). As expected, TCI increased gradually along each treatment stage due to the removal of hemicellulose and lignin. Higher TCI values were obtained for the untreated coir fibre and its resulting treated samples as compared to those obtained for SCB treated under similar alkaline treatment conditions (run A). It may be possible that coir fibre displayed higher cellulose crystallinity when compared with SCB, and SCB may have more amorphous regions in its cellulose structure (Poletto et al., 2014). This was in fact indicated by the higher LOI value of untreated coir as compared to bagasse, which meant that the band of the IR spectra of untreated coir was more towards 1420 cm^{-1}. This implied that the amounts of amorphous cellulose decreased and that coir fibre had a significantly higher amount of crystalline cellulose (Kljun et al., 2011).

LOI is related to the overall degree of order in cellulose (Beltramino et al., 2016). It gives the ratio of the band associated with crystalline structure (1420 cm^{-1}) to the band related to the amorphous region (898 cm^{-1}). Higher LOI can be attributed to cellulose chains closely packed together resulting in a lower amorphous content (Ornaghi et al., 2014). It was observed that untreated bagasse and coir fibres had higher LOI than the treated samples. This decrease in LOI suggested that there had been increased exposure of the cellulose surface upon treatment of the natural fibres that would theoretically facilitate

Table 3 Crystallinity indices of the untreated and treated bagasse and coir samples

Sample	TCI	LOI	HBI
Sugarcane Bagasse (SCB)			
Untreated SCB (UB)	0.57	1.00	3.25
Run *A* (alkaline treatment conditions: 2 wt%, 16 h, 90 °C)			
Alkali treated SCB (AB- *A*)	0.71	0.52	2.00
Bleached SCB (BB-*A*)	0.70	0.59	1.81
NC (NCB-*A*)	0.85	0.63	2.09
Run *B* (alkaline treatment conditions: 17.5 wt%, 1.5 h, 90 °C)			
Sample	TCI	LOI	HBI
Alkali treated SCB (AB-*B*)	0.78	0.67	2.07
Bleached SCB (BB-*B*)	0.81	0.60	1.67
NC (NCB-*B*)	0.76	0.88	2.47
Coir fibre (CF)			
Run *A* (alkaline treatment conditions: 2 wt%, 16 h, 90 °C)			
Sample	TCI	LOI	HBI
Untreated CF (UC-*A*)	0.77	2.00	4.38
Alkali treated CF (AC-*A*)	0.96	1.55	3.18
Bleached CF (BC-*A*)	1.15	1.25	2.13
NC (NC-*A*)	1.03	1.13	2.11

cellulose hydrolysis (Spiridon et al., 2011). Similar observations were made by Beltramino et al. (2016), whereby the authors performed enzymatic hydrolysis on untreated cotton linters, which led to an increased exposure of the cellulose surface and ultimately caused a decrease of about 34% in the LOI. The results hence showed that as each treatment was done, the non-cellulosic constituents and amorphous regions were being removed, exposing the crystalline cellulose which was then synthesized to nanocellulose having a higher degree of crystallinity. Nanocellulose derived from coir fibre showed the highest TCI and LOI values, hence indicating highest degree of crystallinity and a more ordered cellulose structure as compared to that of SCB. It was therefore expected that composite films prepared from coir nanocellulose will exhibit higher tensile strength. HBI indicates the chain mobility and bond distance and is thus connected to crystallinity (Poletto et al., 2013). It was observed that HBI values of both fibres decreased after alkaline treatment and that nanocellulose from coir fibre under run *A* had a lower HBI compared to nanocellulose extracted from SCB under run *B*. This result seemed to indicate that the natural fibres have higher cellulose crystallinity than the treated samples and that nanocellulose extracted from coir fibre had lower cellulose crystallinity when compared to nanocellulose extracted from SCB. However, a high HBI value does not necessary imply a high cellulose crystallinity since the bands associated with finding HBI namely 3350 and 1318 cm^{-1} also refer to the amount of bound water, which may consequently alter the TCI and LOI results (Poletto et al., 2014).

3.4 Morphological analysis through SEM

The SEM micrograph of untreated bagasse (Fig. 5a) and coir fibres (Fig. 5g) showed that the fibre structures were compact and had a stiff surface due to the presence of the primary wall. An alignment was displayed in the fibre axis direction. The overall surface of both fibres appeared smooth due to the presence of wax and oil.

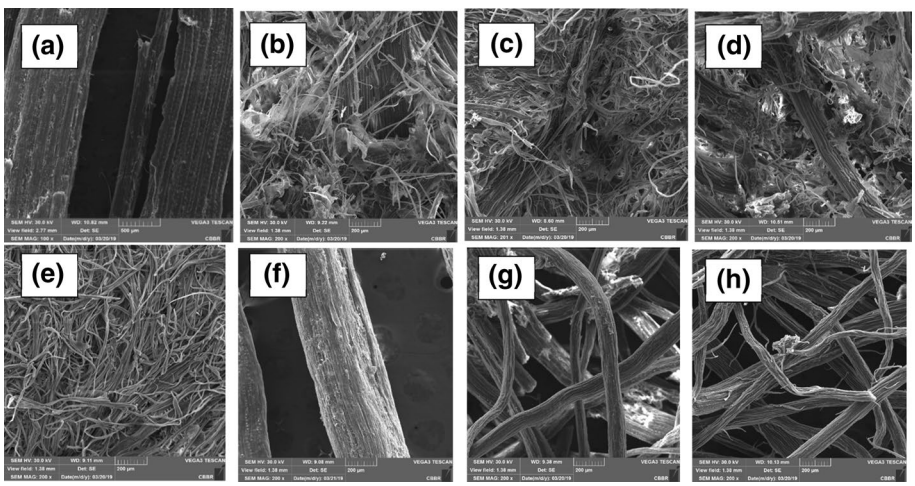

Fig. 5 SEM micrographs of **a** untreated SCB **b** alkali treated SCB at run *A* **c** Bleached SCB at run *A* **d** alkali treated SCB at run *B* **e** Bleached SCB at run *B* **g** untreated CF **h** alkali treated CF at run *A* **i** Bleached CF at run *A*

Upon alkalisation, defibrillation of the fibrous structure occurred due to partial removal of non-cellulosic constituents namely hemicellulose and lignin, resulting in a less compact and disordered structure. As compared to alkali treated SCB extracted under alkaline treatment conditions (run *A*), the fibre bundles of the alkali treated coir fibre were stiffer and more ordered, as shown in Fig. 5h, which may explain the higher LOI value of sample AC-A as compared to that of AB-A in Table 3. Bleaching had further weakened the interaction between hemicellulose, lignin and cellulose, causing fragmentation of fibre bundles into individual fibres, whose diameters were relatively smaller as compared to the untreated fibre. Mandal and Chakrabarty (2011) treated sugarcane bagasse with 17.5 wt% NaOH at boiling temperature for 5 h after bleaching with 0.7 wt% sodium chlorite solution. The resulting SEM micrograph of the pulp after these two treatments showed less defibrillation as compared to the pretreatment conditions studied here. Consequently, the SEM of the nanocellulose extracted by Mandal and Chakrabarty (2011) indicated presence of fibril structure, which remained compact and ordered. On that account, it can be said that the use of optimum treatment conditions can significantly affect the effectiveness of extracting nanocellulose.

The nanocellulose obtained from bagasse appeared as irregular and small circular particles. These spherical or irregular particle shapes may be the result of agglomeration after freeze-drying (Mendes et al., 2015). The nanocellulose particles from coir fibre appeared smaller than those extracted from SCB under similar alkaline treatment conditions (run *A*). Similarly, the CNC from bagasse (run *B*) appeared relatively smaller than that from bagasse (run *A*), which was further observed from the DLS results. However, the SEM images of the nanocellulose samples were not distinct enough to make other precise observations.

3.5 Relative comparison of particle size distribution of nanocellulose from DLS analysis

During acid hydrolysis, there is random cleavage of the cellulose molecular chains and this causes a considerable variation in the dimensions of the resulting nanocellulose particles (Basu et al., 2018). DLS analysis, which measures hydrated particles in suspension, was used to provide a relative comparison between the average size of CNC from bagasse and coir. It was found, as shown in Fig. 6, that the average particle size, expressed as a function of particle diameter, of nanocellulose particles extracted from coir fibres under run *A* was 137.3 nm and that for bagasse, larger sized particles were obtained, namely around 48 μm and 347.8 nm produced under runs *A* and *B,* respectively. One plausible explanation for the particle size differences may be related to the transformation of cellulose I into cellulose II. Proper transformation of cellulose I into II is normally achieved with higher NaOH concentration of at least 10 wt%, according to Dinand et al. (2002). Hence, CNC produced from bagasse under run A may contain more of cellulose I and a smaller portion of cellulose II as compared to CNC produced from bagasse under run *B*. On the other hand, given that the chemical composition of coir is different from bagasse, even under run *A* there seemed to be relatively more cellulose II in coir as compared to bagasse. This was indicated in Fig. 4, where the band at 895 cm^{-1}, associated with cellulose II, is more prominent for coir as compared to bagasse.

The results also suggested that possible agglomeration of particles may have occurred after freeze drying and then rehydration in aqueous medium. Zhou et al. (2012) obtained average particle size of nanocellulose up to 623 nm which was attributed to the rapid agglomeration of nanocellulose in water suspension. This issue had also been reported

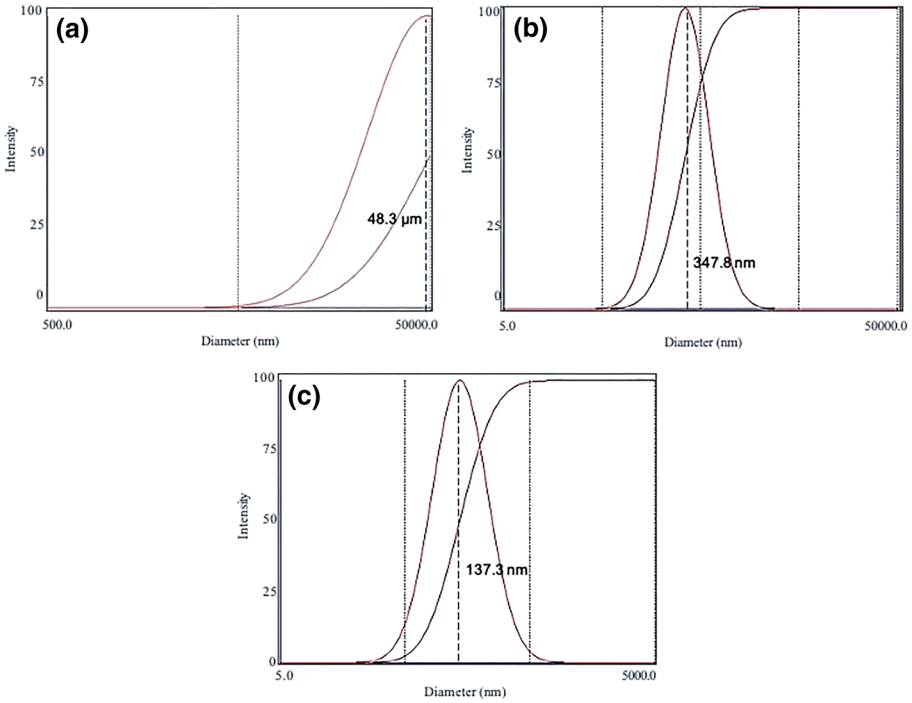

Fig. 6 Particle size distribution of the nanocellulose samples from **a** bagasse (run *A*), **b** bagasse (run *B*) and **c** coir (run *A*)

by Mendes et al. (2015) whereby particles in the range of 1–10 µm had been obtained. They reported that after applying spray drying, the nanocellulose aqueous dispersions produced particle agglomerates with spherical and irregular shapes. Abdelwahed et al. (2006) outlined that freeze drying of nanocellulose particles can impact the stabilisation of the nanoparticles upon redispersion in water. During freezing of the nanocellulose suspensions, ice crystallization can impose severe mechanical stresses on the nanoparticles. This may be resolved by adding special excipients such as glucose, sucrose and mannitol to the nanocellulose suspension before freezing. These sugars immobilized the nanoparticles within a glass-like structure at a specific temperature known as the glass transition temperature (T_g'), hence reducing any freezing or drying stress and also improving the stability of the nanocellulose suspension upon storage (Abdelwahed et al., 2006). Therefore, the results indicated that the possibility of agglomerates formation was higher for bagasse nanocellulose sample as compared to coir.

The polydispersity indices (PI) for the analysis of nanocellulose extracted from sugarcane bagasse under runs *A* and *B* were 0.659 and 0.363, respectively, while that for nanocellulose extracted from coir, the PI was 0.296. According to ISO 22412, a polydispersity index > 0.7 indicates a broad size distribution, hence implying that a sample is not appropriate for DLS analysis. In this case, the results demonstrate that the obtained analysis had narrower size distribution and had good uniformity.

3.6 Tensile properties of CNC/PVA composites

As shown in Table 4, tensile strength increased with increase in nanocellulose loading from 0.5 to 2 wt% for nanocomposites prepared from nanocellulose extracted from bagasse produced under runs and, respectively. Upon 2 wt% CNC addition to PVA matrix, the bagasse nanocomposite 2 CNC/PVA (*A*) showed an increase of 127.6% and 28.4% in terms of Young's modulus and tensile strength, respectively. A decrease in elongation was also observed for the latter as 2 wt% CNC was added to PVA, thereby showing a more brittle behaviour. Shrestha et al. (2018) also reported that the incorporation of CNCs in PVA drawn fibres lead to higher brittleness as well as fibrils. These authors further mentioned that the extent of orientation of the fibrils morphology along the PVA CNC composite fibre has a direct bearing on the fibre tensile strength. The increase in tensile strength may be due to the formation of hydrogen bonds between CNC and PVA, thus causing an increase in their interaction. This ultimately led to a restriction in motion and enhancement of the rigidity, thereby decreasing the % elongation at break (Dey et al., 2017; Wu et al., 2015).

As for the bagasse nanocomposite 2 CNC/PVA (*B*), tensile strength increased by 89.2% at 2 wt% CNC addition as compared to pure PVA. However, there was a relatively small decrease in the Young's modulus as CNC (run *B*) loading was increased from 0.5 to 2 wt%. This may be attributed to the significant increase in % elongation upon increase of CNC content from 0.5 to 2 wt%, hence showing that the polymer mobility had increased, which may be a result of broken intermolecular hydrogen bonds. Therefore, this increase in strain accompanied with a significant increase in tensile strength led to a slight decrease in Young's modulus as more CNC was added to the PVA matrix. Shrestha et al. (2018) reported an increase between 100 and 200% (depending on whether the fibres were spun or drawn and also based on the aspect ratio of the CNC) in the tensile strength of the PVA/CNC composite fibre when the CNC loading was increased from 0 to 15%, and a decrease when the CNC loading was further increased to 20 wt%. Similarly, Zhou et al. (2017) investigated the effect of increasing cotton stalk-based CNC loading in the range of 0–7 wt% in PVA matrix and reported that the highest increase in tensile strength was obtained at 3 wt%. This thus demonstrates that addition of nanocellulose, even at low loadings, can significantly improve the mechanical properties of PVA.

Table 4 Tensile test parameters of CNC/PVA film composites at different wt%

Sample	Thickness (mm)	% elongation	Tensile strength (MPa)	Young`s Modulus (MPa)
Pure PVA	0.187 ± 0.012	144.1 ± 1.2	19.4 ± 2.3	11.6
Sugarcane bagasse (runs *A* and *B*)				
0.5 CNC/PVA (*A*)	0.167 ± 0.014	128.9 ± 1.7	23.4 ± 0.9	20.3
2 CNC/PVA (*A*)	0.182 ± 0.018	105.8 ± 1.5	24.9 ± 1.4	26.4
0.5 CNC/PVA (*B*)	0.179 ± 0.023	149.1 ± 0.9	28.6 ± 2.1	20.0
2 CNC/PVA (*B*)	0.163 ± 0.025	187.0 ± 1.3	36.7 ± 1.8	19.5
Coir fibre (run *A*)				
0.5 CNC/PVA (*A*)	0.175 ± 0.020	170.3 ± 0.9	38.2 ± 0.6	23.3
2 CNC/PVA (*A*)	0.182 ± 0.017	173.1 ± 1.1	32.8 ± 1.3	21.8

When using nanocellulose extracted from coir fibre as reinforcement in the PVA matrix, it was observed that the tensile strength and Young's modulus increased by 96.9% and 100.9%, respectively at 0.5 wt% as compared to pure PVA. But as CNC addition was increased to 2 wt%, the tensile strength decreased while % elongation increased slightly, which ultimately led to small decrease in Young`s modulus. This may be attributed to the formation of agglomerates, with increase in nanocellulose loading, causing voids within the composite matrix resulting in slightly poor adhesion of CNC within the polymer (Peng et al., 2013).

On comparing the CNC/PVA composites prepared using nanocellulose extracted from bagasse prepared under runs *A* and *B* respectively, it could be seen that the tensile strengths were higher for CNC/PVA (*B*) as compared to CNC/PVA (*A*). This may be explained by the larger particles in micrometre range that were obtained at extraction under run *A*. This agglomeration of nanoparticles would thus lead to non-uniform particle distribution, hence affecting the strength. On the other hand, for CNC/PVA (*B*), there was relatively less agglomeration due to the smaller particle size and ultimately lower aspect ratio (as observed from the relative comparison of the SEM and DLS analysis of CNC from bagasse under runs *A* and *B*), thus leading to higher tensile strengths. As reported by Shrestha et al. (2018), cotton-based CNC had greater tensile strength in contrast to wood-based CNC at same CNC loading due to the higher aspect ratio of the former.

In terms of the resulting CNC/PVA composites prepared from nanocellulose isolated from sugarcane bagasse and coir under similar conditions (run *A*), it was observed that tensile strengths of the composites of coir were considerably higher as compared to that of that sugarcane bagasse. This may be attributed to the characteristic differences existing between CNCs from sugarcane bagasse and coir. As stated in Sect. 3.3.2, the IR spectra of the nanocellulose isolated from coir displayed greater band intensities at 3300 cm^{-1} and at 1029 cm^{-1}, indicating larger number of hydroxyl groups. This may in turn be associated with an increase in the number of hydrogen bonds formed. In addition, higher TCI value and lower particle size were obtained for nanocellulose derived from coir, implying higher crystallinity degree and less agglomeration thus leading to a greater mechanical improvement.

4 Conclusion

In this study, nanocellulose has been successfully synthesized from sugarcane bagasse and coir fibres. FTIR results showed that the intensity at band 3300 cm^{-1}, associated with hydroxyl groups responsible for intermolecular hydrogen bonding between CNC and PVA, was higher for CNC from coir than that from bagasse extracted under similar conditions. Higher TCI and LOI values were also obtained for CNC from coir as compared to CNC from bagasse. DLS results showed that the smallest average particle size was obtained for CNC sample from coir at 137.3 nm. CNC isolated from bagasse, at initial mercerisation conditions of 17.5 wt% NaOH at 90 °C for 1.5 h were smaller in size at 347.8 nm as compared to the micrometre-ranged particles extracted from bagasse using 2 wt% NaOH at 90 °C for 16 h. This was due to the short band at 895 cm^{-1}, indicating lower content of finer crystallites of cellulose II in bagasse fibres treated with the 2 wt% NaOH at 90 °C for 16 h. These findings led to the resulting PVA/CNC films of coir having higher tensile strengths than those of bagasse produced under similar conditions. At 2 wt% CNC addition, the tensile strength of PVA/CNC film of coir was about 32% higher than that

of bagasse, both prepared under run *A*. This study hence showed that sugarcane bagasse and coir can be potential sources of nanocellulose for the purpose of producing biodegradable composites with high tensile strengths. Such composites can prove to be efficient environment-friendly and sustainable alternatives to synthetic ones for prospective applications including packaging, separation membranes and scaffolds for tissue engineering. As a future recommendation, further characterisation of the nanocomposite film in terms of biodegradability and moisture uptake can be carried out to enhance its performance for the above-mentioned applications.

References

Abdelwahed, W., Degobert, G., Stainmesse, S., & Fessi, H. (2006). Freeze-drying of nanoparticles: Formulation, process and storage considerations. *Advanced Drug Delivery Reviews, 58*(15), 1688–1713. https://doi.org/10.1016/j.addr.2006.09.017

Abdullah, N. A., Rani, M. S. A., Mohammad, M., Sainorudin, M. H., Asim, N., Yaakob, Z., Razali, H., & Emdadi, Z. (2021). Nanocellulose from agricultural waste as an emerging material for nanotechnology applications—An overview. *Polimery, 66*, 157–168.

Abitbol, T., Rivkin, A., Cao, Y., Nevo, Y., Abraham, E., Ben-Shalom, T., Lapidot, S., & Shoseyov, O. (2016). Nanocellulose, a tiny fiber with huge applications. *Current Opinion in Biotechnology, 39*, 76–88. https://doi.org/10.1016/j.copbio.2016.01.002

Abraham, E., Deepa, B., Pothan, L. A., Jacob, M., Thomas, S., Cvelbar, U., & Anandjiwala, R. (2011). Extraction of nanocellulose fibrils from lignocellulosic fibres: A novel approach. *Carbohydrate Polymers, 86*, 1468–1475. https://doi.org/10.1016/j.carbpol.2011.06.034

Abraham, E., Deepa, B., Pothen, L. A., Cintil, J., Thomas, S., John, M. J., Anandjiwala, R., & Narine, S. S. (2013). Environmental friendly method for the extraction of coir fibre and isolation of nanofibre. *Carbohydrate Polymers, 92*(2), 1477–1483. https://doi.org/10.1016/j.carbpol.2012.10.056

Alexandre, M., & Dubois, P. (2000). Polymer-layered silicate nanocomposites: Preparation, properties and uses of a new class of materials. *Materials Science and Engineering R: Reports, 28*(1–2), 1–63. https://doi.org/10.1016/S0927-796X(00)00012-7

Asem, M., Nawawi, W. M. F. W., Jimat, D. N. (2018). Evaluation of water absorption of polyvinyl alcohol-starch biocomposite reinforced with sugarcane bagasse nanofibre: Optimization using Two-Level Factorial Design. *IOP Conference Series: Materials Science and Engineering*, 368, 012005. https://doi.org/10.1088/1757-899X/368/1/012005

Basri, W. N. F. W., Daud, H., Lam, M. K., Cheng, C. K., Oh, W. D., Tan, W. N., Shaharun, M. S., Yeong, Y. F., Paman, U., Kusakabe, K., Kadir, E. A., Show, P. L., & Lim, J. W. (2019). A sugarcane-bagasse-based adsorbent employed for mitigating eutrophication threats and producing biodiesel simultaneously. *Processes, 7*(9), 572. https://doi.org/10.3390/pr7090572

Basu, T., Bhowmick, S., & Saha, S. (2018). Facile synthesis and characterization of cellulose nanocrystals from waste sugarcane bagasse. *International Journal of Engineering (IOSRD), 5*(1), 33–41.

Beltramino, F., Roncero, M. B., Torres, A. L., Vidal, T., & Valls, C. (2016). Optimization of sulfuric acid hydrolysis conditions for preparation of nanocrystalline cellulose from enzymatically pretreated fibers. *Cellulose, 23*(3), 1777–1789. https://doi.org/10.1007/s10570-016-0897-y

Benyahia, A., Merrouche, A., Rahmouni, Z. E. A., Rokbi, M., Serge, W., & Kouadri, Z. (2013). Study of the alkali treatment effect of natural fibers on the mechanical behavior of the composite unsaturated polyester-alfa fibers. *Mechanics & Industry, 15*(1), 69–73. https://doi.org/10.1051/meca/2013082

Börjesson, M., & Westman, G. (2015). Crystalline Nanocellulose — Preparation, Modification, and Properties. *Cellulose - Fundamental Aspects and Current Trends*, 159–191. https://doi.org/10.5772/61899

Chen, M.-J., Zhang, X.-Q., Liu, C.-F., & Shi, Q.-S. (2016). Homogeneous modification of sugarcane bagasse by graft copolymerization in ionic liquid for oil absorption application. *International Journal of Polymer Science*. https://doi.org/10.1155/2016/6584597

Ciolacu, D., Ciolacu, F., & Popa, V. (2011). Amorphous cellulose—Structure and characterization. *Cellulose Chemistry and Technology, 45*(1), 13–21.

Costa, L. A., Fonseca, A. F., Pereira, F. V., & Druzian, J. I. (2015). Extraction and characterization of nanocellulose from corn stover. *Materials Today: Proceedings., 2*(1), 287–294. https://doi.org/10.1016/j.matpr.2015.04.045

Dai, H., Ou, S., Huang, Y., & Huang, H. (2018). Utilization of pineapple peel for production of nanocellulose and film application. *Cellulose, 25*(3), 1743–1756. https://doi.org/10.1007/s10570-018-1671-0

de Carvalho Mendes, C. A., Ferreira, N. M., Furtado, C. R., & de Sousa, A. M. (2015). Isolation and characterization of nanocrystalline cellulose from corn husk. *Materials Letters, 148*, 26–29. https://doi.org/10.1016/j.matlet.2015.02.047

Dey, D., Selvam, S. P., Kumar, M. M., Sadiku, E. R., & Dey, A. (2017). Mechanical and structural characterization of eco-friendly films prepared using poly(vinyl alcohol), cellulose nanocrystals and chitosan nanoparticle blend. *Asian Journal of Chemistry, 29*(10), 2254–2258.

Dinand, E., Vignon, M., Chanzy, H., & Heux, L. (2002). Mercerization of primary wall cellulose and its implication for the conversion of cellulose I→cellulose II. *Cellulose, 9*(1), 7–18. https://doi.org/10.1023/A:1015877021688

Duchemin, B. J. C. (2015). Mercerisation of cellulose in aqueous NaOH at low concentrations. *Green Chemistry, 17*, 3941–3947. https://doi.org/10.1039/C5GC00563A

Fatmawati, A., Agustriyanto, R., & Liasari, Y. (2013). Enzymatic hydrolysis of alkaline pretreated coconut coir. *Bulletin of Chemical Reaction Engineering and Catalysis, 8*, 34–39. https://doi.org/10.9767/bcrec.8.1.4048.34-39

Feng, Y. H., Cheng, T. Y., Yang, W. G., Ma, P. T., He, H. Z., Yin, X. C., & Yu, X. X. (2018). Characteristics and environmentally friendly extraction of cellulose nanofibrils from sugarcane bagasse. *Industrial Crops and Products, 111*, 285–291. https://doi.org/10.1016/j.indcrop.2017.10.041

Hafemann, E., Battisti, R., Marangoni, C., & Machado, R. A. F. (2019). Valorization of royal palm tree agroindustrial waste by isolating cellulose nanocrystals. *Carbohydrate Polymers, 218*, 188–198. https://doi.org/10.1016/j.carbpol.2019.04.086

Ilyas, R. A., Sapuan, S. M., Asyraf, M. R. M., Dayana, D. A. Z. N., Amelia, J. J. N., Rani, M. S. A., Norrrahim, M. N. F., Nurazzi, N. M., Aisyah, H. A., Sharma, S., Ishak, M. R., Rafidah, M., & Razman, M. R. (2021). Polymer composites filled with metal derivatives: A review of flame retardants. *Polymers, 13*, 1701. https://doi.org/10.3390/polym13111701

International Renewable Energy Agency. (2018). *Renewable power generation costs in 2017. Key findings and executive summary*. Retrieved March, 27, 2019, from https://www.irena.org/-/media/Files/IRENA/Agency/Publication/2018/Jan/IRENA_2017_Power_Costs_2018_summary.pdf?la=en&hash=6A74B8D3F7931DEF00AB88BD3B339CAE180D11C3

Jahan, Z., Niazi, M. B. K., & Gregersen, Ø. W. (2018). Mechanical, thermal and swelling properties of cellulose nanocrystals/PVA nanocomposites membranes. *Journal of Industrial and Engineering Chemistry, 57*, 113–124. https://doi.org/10.1016/j.jiec.2017.08.014

Jayaramudu, T., Ko, H.-U., Kim, H. C., Kim, J. W., Muthoka, R. M., & Kim, J. (2018). Electroactive hydrogels made with polyvinyl alcohol/cellulose nanocrystals. *Materials, 11*, 1615. https://doi.org/10.3390/ma11091615

Kargarzadeh, H., Ahmad, I., Abdullah, I., Dufresne, A., Zainudin, S. Y., & Sheltami, R. M. (2012). Effects of hydrolysis conditions on the morphology, crystallinity, and thermal stability of cellulose nanocrystals extracted from kenaf bast fibers. *Cellulose, 19*, 855–866. https://doi.org/10.1007/s10570-012-9684-6

Khai, D. M., Nhan, P. D., & Hoanh, T. D. (2017). An investigation of the structural characteristics of modified cellulose from acacia pulp. *Vietnam Journal of Science and Technology, 55*(4), 452.

Kljun, A., Benians, T., Goubet, F., Meulewaeter, F., Knox, P., & Blackburn, R. (2011). Comparative analysis of crystallinity changes in cellulose I polymers using ATR-FTIR, X-ray diffraction, and carbohydrate-binding module probes. *Biomacromolecules, 12*(11), 4121–4126. https://doi.org/10.1021/bm201176m

Liu, Y. (2013). Recent progress in fourier transform infrared (FTIR) spectroscopy study of compositional, structural and physical attributes of developmental cotton fibers. *Materials, 6*(1), 299–313. https://doi.org/10.3390/ma6010299

Majid, A. M. A., Mesni, M. S., Raffe, A. H. M., Mohamed, A. H., Ahmad, N. M., & Ghazali, S. A. I. S. M. (2017). Optimization condition of isolation cellulose nanofibrils using NaOH alkaline treatment. *International Journal of Agriculture, Forestry and Plantation, 5*, 45–51.

Ministry of Environment, Solid Waste Management and Climate Change. (2021). *Budget 2021–2022*. Retrieved July, 12, 2021, from https://environment.govmu.org/Pages/Index.aspx

Mandal, A., & Chakrabarty, D. (2011). Isolation of nanocellulose from waste sugarcane bagasse (SCB) and its characterization. *Carbohydrate Polymers, 86*(3), 1291–1299. https://doi.org/10.1016/j.carbpol.2011.06.030

Mauritius Meteorological Services. (2021). *Climate change*. Retrieved July 12, 2021, from http://metservice.intnet.mu/climate-services/climate-change.php

Mauritius Sugar Syndicate. (2018). *Report and Statement Of Account 2017–2018*. Retrieved December 20, 2018, from http://www.mauritiussugar.mu/index.php/en/annual-report.html

Mohomane, S. M., Linganiso, L. Z., Buthelezi, T., & Motaung, T. E. (2017). Effect of extraction period on properties of sugarcane bagasse and softwood chips cellulose. *Wood Research, 62*, 8.

Mtibe, A., Linganiso, L. Z., Mathew, A. P., Oksman, K., John, M. J., & Anandjiwala, R. D. (2015). A comparative study on properties of micro and nanopapers produced from cellulose and cellulose nanofibres. *Carbohydrate Polymers, 118*, 1–8. https://doi.org/10.1016/j.carbpol.2014.10.007

Nasir, M., Hashim, R., Sulaiman, O., & Asim, M. (2017). Nanocellulose: Preparation methods and applications. In M. Jawaid, S. Boufi, & A. H. P. S. Khalil (Eds.), *Cellulose-reinforced nanofibre composites. Woodhead publishing series in composites science and engineering*. Woodhead Publishing.

Omnicane, 2017. *Omnicane Integrated Report 2017*. Retrieved December 20, 2019, from: http://www.omnicane.com/sites/default/files/articlepdf/2017_omnicane_integrated_report_website.pdf

Ornaghi, H. L., Poletto, M., Zattera, A. J., & Amico, S. C. (2014). Correlation of the thermal stability and the decomposition kinetics of six different vegetal fibers. *Cellulose, 21*(1), 177–188. https://doi.org/10.1007/s10570-013-0094-1

Park, S., Baker, J. O., Himmel, M. E., Parilla, P. A., & Johnson, D. K. (2010). Cellulose crystallinity index: measurement techniques and their impact on interpreting cellulase performance. *Biotechnology for Biofuels*. https://doi.org/10.1186/1754-6834-3-10

Peng, J., Srithep, Y., Sabo, R. C., Pilla, S., Peng, X. F., Turng, L. S., & Clemons, C. M. (2013). Fabrication and characterization of polyvinyl alcohol (PVA)/nanofibrillated cellulose (NFC) filaments.

Poletto, M., Pistor, V., & Zattera, A. J. (2013). Structural characteristics and thermal properties of native cellulose. *Cellulose-Fundamental Aspects*. https://doi.org/10.5772/50452

Poletto, M., Ornaghi, J. H. L., & Zattera, A. J. (2014). Native cellulose: Structure, characterization and thermal properties. *Materials, 7*, 6105–6119. https://doi.org/10.3390/ma7096105

Rasheed, M., Jawaid, M., Parveez, B., Zuriyati, A., & Khan, A. (2020). Morphological, chemical and thermal analysis of cellulose nanocrystals extracted from bamboo fibre. *International Journal of Biological Macromolecules, 160*, 183–191. https://doi.org/10.1016/j.ijbiomac.2020.05.170

Rencoret, J., Ralph, J., Marques, G., Gutiérrez, A., Martínez, Á. T., & Del Río, J. C. (2013). Structural characterization of lignin isolated from coconut (*Cocos nucifera*) coir fibers. *Journal of Agriculture and Food Chemistry, 61*, 2434–2445. https://doi.org/10.1021/jf304686x

Shrestha, S., Montes, F., Schueneman, G. T., Snyder, J. F., & Youngblood, J. P. (2018). Effects of aspect ratio and crystal orientation of cellulose nanocrystals on properties of poly (vinyl alcohol) composite fibers. *Composites Science and Technology., 167*, 482–488.

Spiridon, I., Teaca, C. A., & Bodîrlău, R. (2011). Structural changes evidenced by FTIR spectroscopy in cellulose materials after pre-treatment with ionic liquid and enzymatic hydrolysis. *BioResources, 6*(1), 400–413.

Srivastava, K. R., Dixit, S., Pal, D. B., Mishra, P. K., Srivastava, P., Srivastava, N., Hashem, A., Alqarawi, A. A., & Abd Allah, E. F. (2021). Effect of nanocellulose on mechanical and barrier properties of PVA–banana pseudostem fiber composite films. *Environmental Technology and Innovation, 21*, 101312. https://doi.org/10.1016/j.eti.2020.101312

TrendEconomy. (2021). Mauritius | Imports and Exports | World | Vegetables provisionally preserved, but unsuitable in that state for immediate consumption | Value (US$) and Value Growth, YoY (%) | 2009 - 2020. Retrieved July 12, 2021, from https://trendeconomy.com/data/h2/Mauritius/0711

Trifol, J., Sillard, C., Plackett, D., Szabo, P., Bras, J., & Daugaard, A. E. (2016). Chemically extracted nanocellulose from sisal fibres by a simple and industrially relevant process. *Cellulose*. https://doi.org/10.1007/s10570-016-1097-5

Wulandari, W. T., Rochliadi, A., & Arcana, I. M. (2016). Nanocellulose prepared by acid hydrolysis of isolated cellulose from sugarcane bagasse. *IOP Conference Series: Materials Science and Engineering*, 107, 012045. https://doi.org/10.1088/1757-899X/107/1/012045

Wu, G., Liu, D., Liu, G., Chen, J., Huo, S., & Kong, Z. (2015). Thermoset nanocomposites from waterborne bio-based epoxy resin and cellulose nanowhiskers. *Carbohydrate Polymers, 127*, 229–235. https://doi.org/10.1016/j.carbpol.2015.03.078

Yadav, A., Bagotia, N., Sharma, A. K., & Kumar, S. (2021). Advances in decontamination of wastewater using biomass-basedcomposites: A critical review. *Science of the Total Environment, 784*, 147108. https://doi.org/10.1016/j.scitotenv.2021.147108

Yu, K. L., Chen, W.-H., Sheen, H.-K., Chang, J.-S., Lin, C.-S., Ong, H. C., Show, P. L., Ng, E.-P., & Ling, T. C. (2020b). Production of microalgal biochar and reducing sugar using wet torrefaction with microwave-assisted heating and acid hydrolysis pretreatment. *Renewable Energy, 156*, 349–360. https://doi.org/10.1016/j.renene.2020.04.064

Yu, K. L., Chen, W.-H., Sheen, H.-K., Chang, J.-S., Lin, C.-S., Ong, H. C., Show, P. L., & Ling, T. C. (2020a). Bioethanol production from acid pretreated microalgal hydrolysate using microwave-assisted heating wet torrefaction. *Fuel, 279*, 118435. https://doi.org/10.1016/j.fuel.2020.118435

Yu, S., Sun, J., Shi, Y., Wang, Q., Wu, J., & Liu, J. (2021). Nanocellulose from various biomass wastes: Its preparation and potential usages towards the high value-added products. *Environmental Science Ecotechnology, 5*, 100077. https://doi.org/10.1016/j.ese.2020.100077

Zhao, X. B., Wang, L., & Liu, D.-H. (2008). Peracetic acid pretreatment of sugarcane bagasse for enzymatic hydrolysis: A continued work. *Journal of Chemical Technology and Biotechnology, 83*, 950–956. https://doi.org/10.1002/jctb.1889

Zhou, Y. M., Fu, S. Y., Zheng, L. M., & Zhan, H. Y. (2012). Effect of nanocellulose isolation techniques on the formation of reinforced poly(vinyl alcohol) nanocomposite films. *Express Polymer Letters, 6*, 794–804. https://doi.org/10.3144/expresspolymlett.2012.85

Zhou, L., He, H., Jiang, C., Ma, L., & Yu, P. (2017). Cellulose nanocrystals from cotton stalk for reinforcement of poly(vinyl alcohol) composites. *Cellulose Chemistry and Technology, 51*, 109–119.